Università degli Studi di Padova

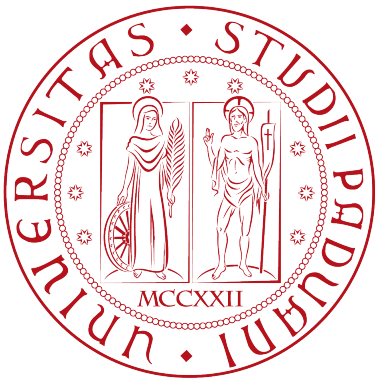

Facoltà di Ingegneria
Dipartimento di Ingegneria dell'Informazione

Corso di Laurea in Ingegneria Biomedica

Tesi di Laurea

Stability Analysis and Design of a PID Controller for an International Moth Class Vessel

Relatore: Prof. Augusto Ferrante

Laureando:
Filippo Santi
1194102

Anno Accademico 2021/2022

Abstract

In this thesis a stability assessments and dynamic simulations in relation to a Moth Class hydrofoiling sailboat, as exemplified by the Banfi prototype, are investigated by means of classical control methods. The International Moth is a single-handed dinghy, which, while moving forward, uses two T-foils to lift the hull above the water. The model is developed on the basis of simple assumptions, semi-empirical methods and the available input data was processed through XFLR5[12]. Stability assessments are carried out with the help of the small disturbance theory, by analysing the eigenvalues and modes of the linearised dynamic system. Then, using the a proposal for a pitch displacement autopilot is made, with the purpose of improving the craft's dynamics. Finally, with the help of Matlab [13] software, the dynamic behaviour of the simplified linearised system faced with canonical reference inputs, such as step and ramp inputs, is simulated to evaluate the stability of the International Moth when fitted with different controllers for a pitch displacement autopilot.

Abstract

In questo elaborato si è valutata, sfruttando gli strumenti froniti dalla teroia dei controlli automatici, la stabilità di un imbarcazione da regata appartenente alla International Moth Class Association, in particolare si è usato l'esempio del prototipo Banfi, progettato dal team studentesco MetisVela UniPD. Le imbarcazioni appartenenti a questa classe si distinguono per la presenza di due T-foil (appendice composta da una sezione verticale e una orizzontale) che generano la portanza idrodinamica necessaria a sollevare lo scafo al di sopra dell'acqua.

Il modello è sviluppato a posteriori di alcune semplici assunti , utilizzando anche risultati empirici. Tutti i dati a disposizione sono stati processati attraverso il software di simulazione XFLR5 [12]. L'analisi di stabilità è stata effettuata ricorrendo alla teoria delle piccole perturbazioni, analizzando gli autovalori e i modi del moto del sistema dinamico lineare.

Infine, utilizzando il software Matlab [13], si è simulata la risposta al bechheggio del sistema linearizzato quando riceve input canonici, quali gradino e rampa, allo scopo di valutare l'efficacia di diversi controllori di beccheggio.

Contents

Introduction

Sailing is an activity that dates back in millennia and has accompanied mankind in some of its most daring adventures. At present, maritime transportation accounts for the vast majority of long-range transportation and is done mainly by means of diesel internal combustion generators coupled with electrical motors. Sailing has become a more leisure-oriented activity, taking the connotation of an extreme sport when it comes to acrobatic dinghies and foilers. With the latter expression we indicate all those sailboats which are fitted with winglike appendages whose sole purpose is to generate a lift force and proceed to heave the hull of the boat out of the water. This flight configuration allows the boat to improve its efficiency greatly since it reduces the wet surface of the vessel, thus reducing hydrodynamic drag. As a matter of fact, foilers rely on the hull's buoyancy merely for safety purposes and to achieve floating before takeoff. In the wide panorama of sailing sports, the International Moth Class has had quite a success among single-crew foilers, becoming the vessel of choice for professional and semi-professional sailors. The International Moth Class differs from other sailing classes mainly for its few design restrictions [9], making it very prone to change and innovation. This has led to it being one of the first and most proficient classes ever on which hydrofoils have been implemented,as far back as the early 2000s. At present, these dinghies are achieving speeds as high as 36.5 knots thanks to the submerged foiling appendages which allow them to fly above the water without displacing any, or very little, while doing so. In the past a notorious effort has been put into the development of foil profiles to best suite the requisites of foiling dinghies belonging to the International Moth Class, but little has been done in the way of stability assessment and control. In particular, designers new to the foiling environment would find helpful to have an intuitive guide that explains the underlying correlation between flight qualities and design choices. The case of study is a prototype under development from the MétisVela UniPD[**?**] student project for the SuMoth [11] competition, and measurements, estimates and inertial properties have been derived for such prototype.

Figure 1: International Moth Class vessel in the act of foiling

1 Purpose and aim

The purpose of this work is to asses the longitudinal stability of the a foiling sailboat from the International Moth Sailing Association class. Vessels belonging to this class display a typical symmetrical hydrofoil planeform, in analogy to what can be observed in STOL (Short Take Off and Landing) and other commercial aircraft, still substantially differing having just one control surface on the forward mounted wing.

The aim is to accurately describe the vessel, its geometric and aerodynamic characteristics through longitudinal stability coefficients. The latter are obtained with the help of the XFLR5 simulation software and have been organised into stability matrices, necessary for state-space modeling. Most of the methods and findings used are derived from aeronautical engineering and have been adjusted to the purpose of this study.

The analysis of the dynamics of the vessel is done by means of the small disturbance theory and a Simulink representation of the model is developed from transfer functions.

In the last section a proposal was developed for a PID controller to be integrated in a pitch displacement autopilot.

2 Aerodynamic principles

Moth Class vessels make use of two different fluids to achieve flight. Air, through the wind's interaction with the sail provides the propulsive thrust and some heeling moment, much as can be observed in conventional sailboats.This interaction can be very difficult to model satisfying way and thus will be overlooked in this work. Water, on the other hand, is responsible for the most notable forces and moments to act on the craft. Due to the different properties of the two fluids, and the pitching moment of the water-induced effects on the craft, we will focus on the contribution of the below-the-waterline hydrofoils.

2.1 Reference system and key variations

For the purpose of simplicity all variations are described with reference to the Center of Gravity of the vessel. The following illustration shows the main movements of the craft and will be used in the mathematical description of the system.

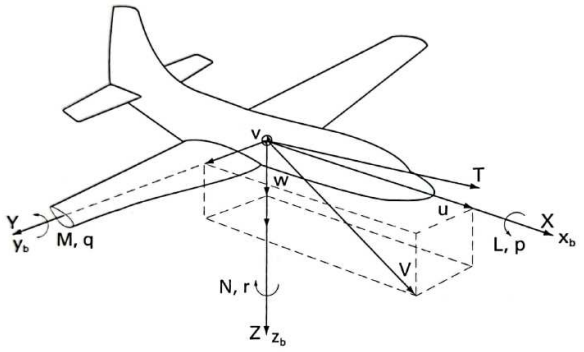

	Roll Axis x_b	Pitch Axis y_b	Yaw Axis z_b
Angular rates	p	q	r
Velocity components	u	v	w
Aerodynamic force components	X	Y	Z
Aerodynamic moment components	L	M	N
Moment of inertia about each axis	I_x	I_y	I_z
Products of inertia	I_{yz}	I_{xz}	I_{xy}

Figure 2: Flight parameters

2.2 Aerodynamic Nomenclature

The nomenclature used is largely borrowed from aeronautics, with the main appendages been named (from aft to bow, down up):

1. Rudderfoil (horizontal wing that provides lift to the rear part of the boat)
2. Rudderboard (vertical wing on which the rudderfoil is fixed, provides steering capabilities)
3. Mainfoil (provides the main lift forces to the boat, has an actuator connected to a moving flap posistioned on the trailing edge)
4. Daggerboard (vertical wing on which the mainfoil is mounted, provides roll stability to the craft)

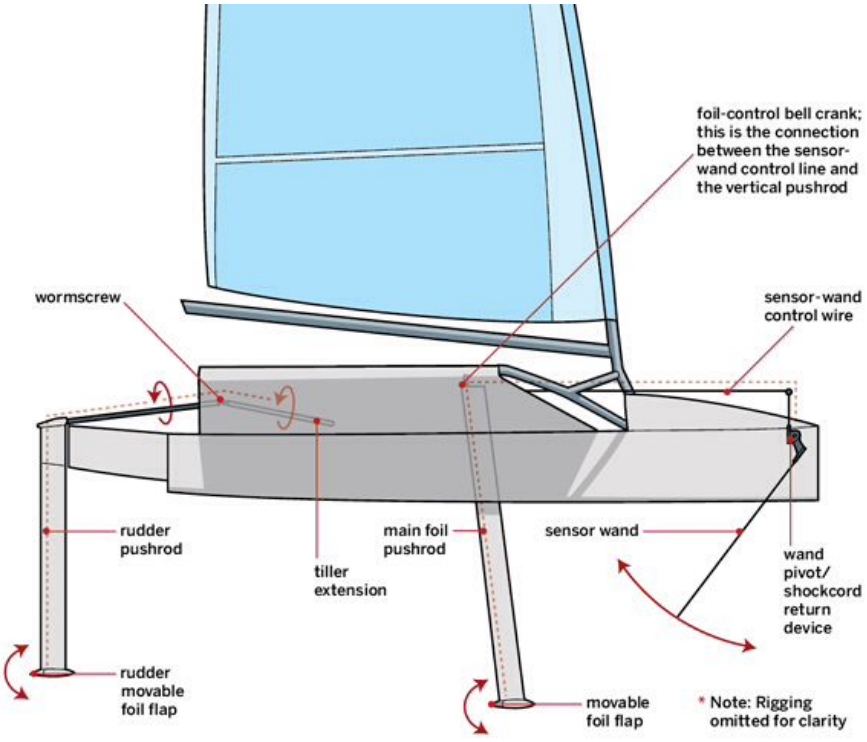

Figure 3: Foling Moth vessel schematic configuration

The aerodynamic profiles employed in this design are the following:

- NACA 0012
- NACA 63012A (rudderfoil)

- NACA 63415 (mainfoil)
- Wortmann FX60100 (mainfoil)

The NACA63415 and Wortmann FX60100 profiles have been used to build a wing of 1m span, with 0.11m and 0.035m of chord at the root and at the tip respectively. The NACA63415 was used maily in the central region to support the intersection with the mast (daggerboard). The NACA63012 was used to build a wing of 0.7m span, with 0.06m and 0.035m of chord at the root and at the tip respectively.

2.3 Simulation parameters

The parameters on which aerodynamic simulations have been built are those for salted water at standard reference conditions (STP), with a density $\rho = 1029\frac{kg}{m^3}$ and a cinematic viscosity of $\nu = 1e-06\frac{m^2}{s}$

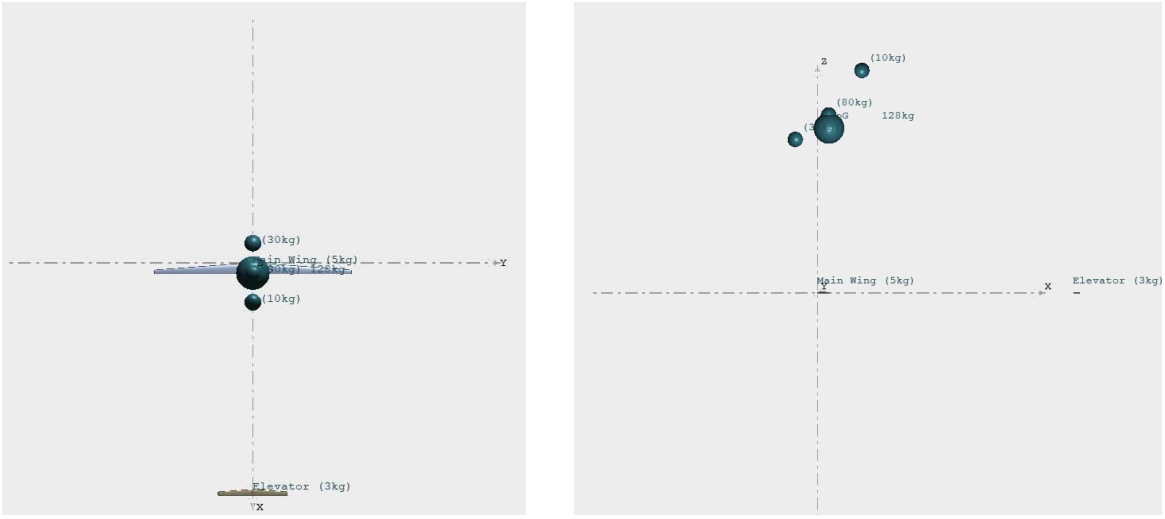

Figure 4: (a) Top view of the mass distribution (b) Left-side view of the mass distributions

3 Static Stability and Control

3.1 Definition of Static Stability

Static stability is the tendency of the system to return to its equilibrium state after a disturbance. The state of equilibrium of the vessel can be defined as the state in which there are no moments or forces acting on the center of gravity of the system ($C_{m_{cg}} = 0$), and can be achieved by flying at trim condition.

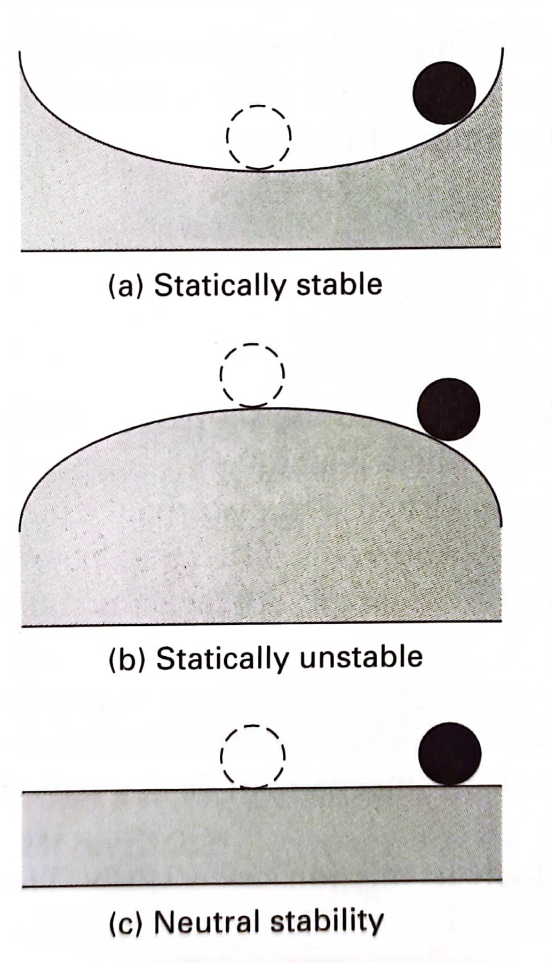

Figure 5: Representation of different static stability properties

3.2 Longitudinal Static Stability

3.2.1 Definition of Longitudinal Static Stability

To attain static stability a restoring moment must be developed when the craft is displaced from its equilibrium point. Supposing a negative moment (pitching-down) affects the vessel, it will be required for it to develop a positive counter-moment to bring itself back to the equilibrium point. Analogously for a "pitching-up" disturbance. To ensure such capability, the aircraft pitching moment curve should have a negative slope.

$$\frac{dC_m}{d\alpha} < 0 \tag{1}$$

or equivalently

$$C_{m_\alpha} < 0 \tag{2}$$

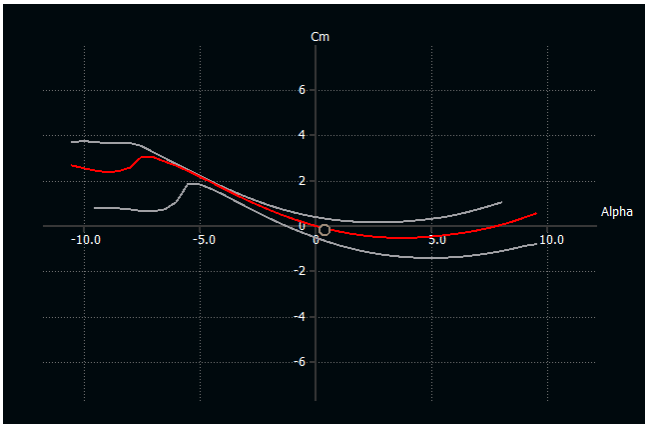

Figure 6: Cm plot for the case study

3.2.2 Contribution of the Craft's Components

In an aircraft wing, fuselage, tail and propulsion all contribute to the planes pitching moment curve and it is the in designer's interest to discriminate the different contributions. For the purpose of our study the hull's contribution will be neglected as it flies through a fluid with very different properties than water. The focus will be for the most part on the relationship between the stability coefficients and the geometric and aerodynamic characteristics of the examined vessel.

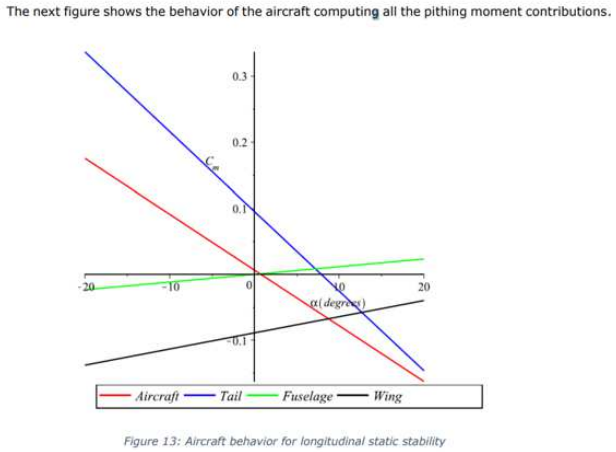

Figure 7: Contribution of the various components on the Cm

3.2.3 Wing Contribution

The contribution to the wing in the plane's static stability can be examined with the help of a simplified representation, showing the wing as it's mean aerodynamic chord.

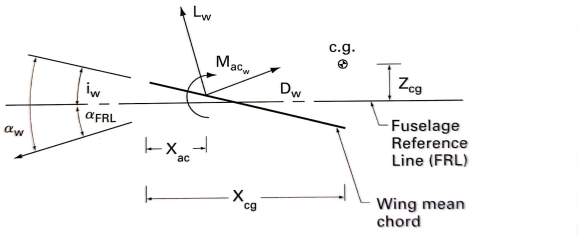

Figure 8: Simplified representation of the main hydrofoil wing's contribution to the pitching moment

The vertical displacement of the center of gravity is noted z_{cg}. The horizontal distance form the wing's leading edge to the aerodynamic center and center of mass are named x_{ac} and x_{cg} respectively. The angle the aerodynamic chord makes with the fuselage reference line is denoted as i_w, angle with which the wing is mounted to the fuselage.

If we sum the moments about the center of gravity, the following equation can be obtained:

$$\begin{aligned} M_{cg_w} = L_w cos(\alpha_w - i_w)[x_{cg} - x_{ac}] + D_w sin(\alpha_w - i_w)[x_{cg} - x_{ac}] \\ + L_w cos(\alpha_w - i_w)[z_{cg}] - D_w sin(\alpha_w - i_w)[z_{cg}] + M_{ac_w} \end{aligned} \tag{3}$$

Assuming that the angle of attack is small, the following approximation can be made:

$$cos(\alpha_w - i_w) = 1; \qquad sin(\alpha_w - i_w) = \alpha_w - i_w; \qquad C_L >> C_D; \tag{4}$$

$Zcg >> 0$ which divided by $\frac{1}{2}\rho V^2 Sc$ yields

$$\begin{aligned} C_{m_{cg_w}} &= C_{L_w} cos(\alpha_w - i_w)(\frac{x_{cg}}{c} - \frac{x_{ac}}{c}) + C_{D_w} sin(\alpha_w - i_w)(\frac{x_{cg}}{c} - \frac{x_{ac}}{c}) \\ &+ C_{L_w} sin(\alpha_w - i_w)[\frac{z_{cg}}{C}] - C_{D_w} cos(\alpha_w - i_w)(\frac{z_{cg}}{c}) + C_{M_{ac_w}} \\ &= C_{L_w}(\frac{x_{cg}}{c} - \frac{x_{ac}}{c}) + C_{L_w}(\alpha_w - i_w)[\frac{z_{cg}}{C}] - C_{D_w}(\frac{z_{cg}}{c}) + C_{M_{ac_w}} \end{aligned} \tag{5}$$

$$C_{m_{cg_w}} = C_{L_w}(\frac{x_{cg}}{c} - \frac{x_{ac}}{c}) + C_{L_w}(\alpha_w - i_w)[\frac{z_{cg}}{C}] - C_{D_w}(\frac{z_{cg}}{c}) + C_{M_{ac_w}} \tag{6}$$

if

$$C_{L_w} = C_{L_{0_w}} + C_{L_{\alpha_w}} \alpha_w \tag{7}$$

and

$$C_{D_w} = C_{D_{0_w}} + C_{D_{\alpha_w}} \alpha_w \tag{8}$$

we then have

$$\begin{aligned} C_{m_{cg_w}} = C_{M_{ac_w}} + (C_{L_{0_w}} + C_{L_{\alpha_w}} \alpha_w)(\frac{x_{cg}}{c} - \frac{x_{ac}}{c}) + \\ (C_{L_{0_w}} + C_{L_{\alpha_w}} \alpha_w)\frac{z_{cg}}{c}(\alpha_w - i_w) - (C_{D_{0_w}} + C_{D_{\alpha_w}} \alpha_w)\frac{z_{cg}}{c} \end{aligned} \tag{9}$$

3.2.4 Aft Tail Contribution

The contribution an horizontal aft tail makes to the vessel lift and pitching moment can be developed with the help of figure, where the mean aerodynamic chord replaces the tail.

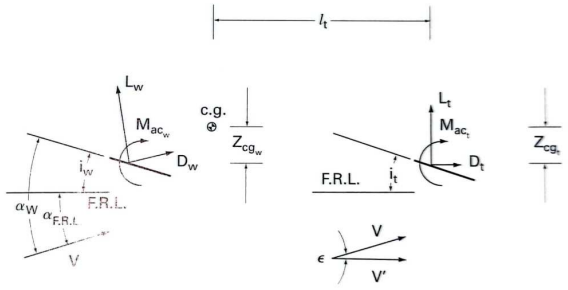

FIGURE 2.9
Aft tail contribution to the pitching moment.

Figure 9: Aft tail contribution

The angle of attack of the tail can be expressed as

$$\alpha_t = \alpha_w - i_w - \epsilon + i_t \tag{10}$$

where ϵ and i_t are the downwash and incidence angle respectively. Assuming small angles and neglecting the tail's drag contribution, the total lift of the wing and tail can be expressed as

$$L = L_w + L_t \tag{11}$$

or

$$C_L = C_{L_w} + \eta \frac{S_t}{S} C_{L_t} \tag{12}$$

where

$$\eta = \frac{Q_t}{Q_w} \tag{13}$$

The value of η can vary in a range $0.8 - 1.2$ depending on the tail's location, but for the purpose of this study we will freely consider this dynamic pressure ratio η to be unitary.

The pitching moment due to the tail can be obtained by summing the moments about the center of gravity.

$$\begin{aligned} M_t = -l_t[L_t cos(\alpha_{FRL} - \epsilon) + D_t sin(\alpha_{FRL} - \epsilon)] \\ -z_{cg}[D_t cos(\alpha_{FRL} - \epsilon) - L_t sin(\alpha_{FRL} - \epsilon)] + M_{ac_t} \end{aligned} \tag{14}$$

Assuming small angles and $C_L >> C_D$ the previous equation reduces to:

$$M_t = -l_t L_t = -l_t \frac{1}{2} \rho V_t^2 S_t \tag{15}$$

$$C_{M_t} = \frac{M_T}{\frac{1}{2}\rho V^2 Sc} = -\frac{l_t S_t}{Sc} \eta C_{L_t} \tag{16}$$

where $V_h = \frac{l_t S_t}{(Sc)}$ is called horizontal tail volume ratio. The coefficient C_{L_t} can be written as:

$$C_{L_t} = C_{L_{\alpha_t}} \alpha_t = C_{L_{\alpha_t}} (\alpha_w - i_w + i_t) \tag{17}$$

where the angle of attack of the tail is written as

$$\alpha_t = \alpha_w - i_w + i_t \tag{18}$$

where no downwash is taken into account. Rewriting the tail contribution yields:

$$\begin{aligned} C_{M_{cg_t}} &= -V_H \eta C_{L_t} \\ C_{M_{cg_t}} &= V_H \eta C_{L_{t_\alpha}} (i_w - i_t - \alpha) \end{aligned} \tag{19}$$

The tail contribution to the static stability of the airplane ($C_{m_{\alpha_t}} < 0$) can be controlled by proper selection of the volume ratio V_H and $C_{L_{\alpha_t}}$.

3.2.5 Elevator Effectiveness

Pitch attitude can be controlled by means of a flap located on the the vessel's forward main wing. When this elevator is deflected, changes in the pitching moment of the vessel occur. The change in the lift can be expressed as follows:

$$\Delta C_L = C_{L_\alpha} \alpha + C_{L_{\delta_e}} \delta_e \tag{20}$$

where

$$C_{L_{\delta_e}} = \frac{dC_L}{d\delta_e} \tag{21}$$

The change in pitching moment acting on the vessel can be also written as

$$\Delta C_m = C_{m_{\delta_e}} \delta_e \tag{22}$$

where

$$C_{m_{\delta_e}} = \frac{dC_m}{d\delta_e} \tag{23}$$

The stability derivative $C_{m_{\delta_e}}$ is called elevator control power. Tle larger the value, the more effective the control is in creating control moment. The complete pitching moment equation yields

$$C_m = C_{m_0} + C_{m_\alpha} \alpha + C_{m_{\delta_e}} \delta_e \tag{24}$$

The derivatives $C_{L_{\delta_e}}$ and $C_{m_{\delta_e}}$ are related to aerodynamic and geometric characteristics. The designer can control the magnitude of the elevator control power by a proper selection of the flap size.

3.3 Definition of Dynamic Stability

The study of dynamic stability is concerned with the time history of the motion of the plant after it is disturbed from its equilibrium point. To achieve dynamic stability static stability needs to first be ensured. The degree of dynamic stability of a system can be specified by the time it takes a disturbance to be reduced to half its original amplitude, in the presence of positive damping, or the time it takes a disturbance to double its original amplitude, if the system were to be negatively damped. In this case, we observe the behaviour of the plant through 4 different state variables, namely $\Delta u, \Delta w, \Delta q, \Delta\theta$. Making use of longitudinal stability derivatives allows to describe accurately the behaviour of the vessel.

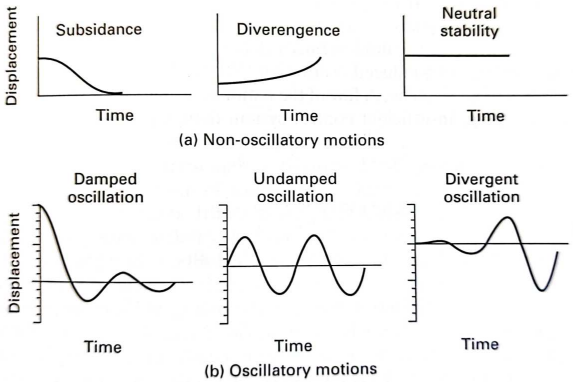

Figure 10: Time evolution of stable (left) and unstable (right) non-oscillatory (top) and oscillatory (bottom) modes of motion

4 Description of the control problem

International Moth class hydro-foiling vessels are required to achieve stable flight at a given height and speed by means of just one control surface positioned on the trailing edge of the main hydrofoil. The design of this flap and an evaluation of its effectiveness have been carried out separately. The description of the vessel's flight can be very complex and yield a set of 6 non-linear, coupled differential equations. Thus, after making some simplifications and having made assumptions on the reference sailing condition, two separate sets of linearised decoupled equations can be developed. The first describes the plane/vessel's longitudinal behaviour, the second describes its lateral behaviour.

4.1 Longitudinal assumptions and Reference Flight Condition

In doing so we assume that the motion of the airplane consists of small deviations from a steady flight condition. For convenience, the reference flight condition is assumed to be symmetric and thrust forces are assumed to remain constant. This resulting in: $v_0 = p_0 = q_0 = r_0 = \psi_0 = \Phi_0 = 0$ Furthermore if the x axis were to be aligned to the direction of the vessel's velocity vector, then $w_0 = 0$.

4.2 Derivation of Mathematical Model

The scalar equations for a rigid body with 6 DOF derived from rational mechanics can be divided in two groups, one representing the force and the second the moments' components and both comprise aerodynamic and gravitational contributions.

Force equations:

$$X - mgS_\theta = m(\dot{u} + qw - rv) \tag{25}$$

$$Y + mgC_\theta S_\phi = m(\dot{v} + ru - pw) \tag{26}$$

$$Z + mgC_\theta C_\phi = m(\dot{w} + pv - qu) \tag{27}$$

Moment equations:

$$L = I_x\dot{p} - I_{xz}\dot{r} + qr(I_z - I_y) - I_{xz}pq \tag{28}$$

$$M = I_y\dot{q} + rp(I_x - I_z) + Ixz(p^2 - r^2) \tag{29}$$

$$N = -I_{xz}\dot{p} + I_z\dot{r} + pq(I_y - I_x) + I_{xz}qr \tag{30}$$

For the purposes of this work the roll rate and yaw rate and their respective rates will be considered to be null, leaving a simplified version of the equation of motion.

Force equations:

$$X - mgS_\theta = m(\dot{u} + qw) \tag{31}$$

$$Y = m\dot{v} \tag{32}$$

$$Z + mgC_\theta = m(\dot{w} - qu) \tag{33}$$

Moment equations:

$$L = 0 \tag{34}$$

$$M = I_y\dot{q} \tag{35}$$

$$N = 0 \tag{36}$$

These force and moments are written in terms of body angular velocities.

5 Small Disturbance Notation

The set of longitudinal equations developed in the previous chapter can be linearised using small disturbance theory. Introducing small-disturbance notation allows us to further simplify the equations of motion. All the variables in the equations of motion are replaced by a reference value, evaluated at reference trim condition, plus a perturbation value.

The X-force equation

$$X - mgsin\Theta = m(\dot{u} + qw - rv) \tag{37}$$

when substituted with the small-disturbance variables gives

$$\begin{aligned} X_0 + \Delta X - mgsin(\theta_0 + \Delta\theta) = \\ m[\frac{d}{dt}(u_0 + \Delta u) + (q_0 + \Delta q)(w_0 + \Delta w) - (r_0 + \Delta r)(v_0 + \Delta v)] \end{aligned} \tag{38}$$

making a trimmed flight condition flight condition assumption, as in

$$w_0 = v_0 = p_0 = q_0 = r_0 = \Phi_0 = \Psi_0 = 0 \tag{39}$$

neglecting products of disturbance, the X equation becomes:
$X_0 + \Delta X - mgsin(\theta_0 + \Delta\theta) = m\Delta\dot{u}$
applying the:
$sin(\theta_0 + \Delta\theta) = sin\theta_0 cos\Delta\theta + sin\Delta\theta cos\theta_0 = sin\theta_0 + \Delta\theta cos\theta_0$
trigonometric identity yields:
$X_0 + \Delta X - mg(sin\theta_0 + \Delta\theta cos\theta_0) = m\Delta\dot{u}$

If all disturbance quantities are set to zero, we have the reference flight condition in the X body direction:
$X_0 - mgsin\theta_0 = 0$
This reduces the X- force equation to:
$\Delta X - mg\Delta\theta cos\theta_0 = m\Delta\dot{u}$
The force ΔX is the variation in aerodynamic forces in the X body direction and can be expressed by means of a Taylor series in terms of the perturbation variables. Virtually these forces and moments could be expressed as a function of all the motion variables, but here only significant terms have been retained.

$$\Delta X = \frac{\partial X}{\partial u}\Delta u + \frac{\partial X}{\partial w}\Delta w + \frac{\partial X}{\partial \delta_e}\Delta\delta_e \tag{40}$$

substituting the formula for ΔX in to the equation of motion yields:

$$\frac{\partial X}{\partial u}\Delta u + \frac{\partial X}{\partial w}\Delta w + \frac{\partial X}{\partial \delta_e}\Delta\delta_e - mg\Delta\theta cos\theta_0 = m\Delta\dot{u} \tag{41}$$

or, dividing through by the mass m:

$$(\frac{d}{dt} - X_u)\Delta u - X_w\Delta w + (gcos\theta_0)\Delta\theta = X_{\delta_e}\Delta\delta_e \tag{42}$$

where $X_u = \partial X/\partial u/m$ and so forth.
The Z-force equation:

$$Z + mgC_\theta = m(\dot{w} - qu) \tag{43}$$

when substituted with the perturbation variables gives:

$$(Z_0 + \Delta Z) + mgcos(\theta_0 + \Delta\theta) = m\frac{d}{dt}(w_0 + \Delta w) - (q_0 + \Delta q)(u_0 + \Delta u) \tag{44}$$

We use the trigonometric identity for which
$cos(\theta_0 + \Delta\theta) = cos\theta_0 cos\Delta\theta - sin\theta_0 sin\Delta\theta = cos\theta_0 - \Delta\theta sin\theta_0$.
Neglecting all perturbations' products and assuming reference flight condition leaves:

$$(Z_0 + \Delta Z) + mgcos(\theta + \Delta\theta) = m\frac{d}{dt}\Delta w - u_0\Delta q \tag{45}$$

Setting all perturbation values to 0 gives once again the reference fight condition

$$Z_0 + mgcos\theta = 0 \tag{46}$$

thus reducing the small-perturbation Z-force equation to:

$$\Delta Z - mg\Delta\theta sin\theta_0 = m\frac{d}{dt}\Delta w - u_0\Delta q \tag{47}$$

In analogy to the previous case, the Z-force can be written as a function of the motion variables, namely:

$$\Delta Z = \frac{\partial Z}{\partial u}\Delta u + \frac{\partial Z}{\partial w}\Delta w + \frac{\partial Z}{\partial q}\Delta q + \frac{\partial Z}{\partial \delta_e}\Delta\delta_e \tag{48}$$

When substituted in the force equation it gives:

$$-\frac{\partial Z}{\partial u}\Delta u + (m\frac{d}{dt} - \frac{\partial Z}{\partial w})\Delta w + mg\Delta\theta sin\theta_0 - u_0\Delta q = \frac{\partial Z}{\partial \delta_e}\Delta\delta_e \tag{49}$$

When divided by the mass m it gives

$$-Z_u\Delta u + [(1 - Z_{\dot{w}})\frac{d}{dt} - Z_w]\Delta w - [(u_0 + Z_q)\frac{d}{dt} - gsin\theta_0]\Delta\theta = Z_{\delta_e}\Delta\delta_e \tag{50}$$

where $Z_u = \partial Z/\partial u/m$ and so forth.

The linear small-disturbance longitudinal set of rigid body equations of motion will then be:

$$(\frac{d}{dt} - X_u)\Delta u - X_w\Delta w + (mgcos\theta_0)\Delta\theta = X_{\delta_e}\Delta\delta_e \tag{51}$$

$$-Z_u\Delta u + [(1 - Z_{\dot{w}})\frac{d}{dt} - Z_w]\Delta w - [(u_0 + Z_q)\frac{d}{dt} - gsin\theta_0]\Delta\theta = Z_{\delta_e}\Delta\delta_e \tag{52}$$

$$-M_u\Delta u - (M_{\dot{w}}\frac{d}{dt} + M_w)\Delta w + (\frac{d^2}{dt^2} - M_q\frac{d}{dt})\Delta\theta = M_{\delta_e}\Delta\delta_e \tag{53}$$

Follows a table with relevant longitudinal derivatives for the study case:

Stability Derivative	Parial derivative form	Numerical value
X_u	$\partial X/\partial u$	-0.2881
Z_u	$\partial Z/\partial u$	-14.34
X_w	$\partial X/\partial w$	5.978
Z_w	$\partial Z/\partial w$	-106.36
$Z_{\dot{w}}$	$\partial Z/\partial \dot{w}$	0
Z_q	$\partial Z/\partial q$	-60.17
M_u	$\partial M/\partial u$	0.3162
M_w	$\partial M/\partial w$	-17.766
$M_{\dot{w}}$	$\partial M/\partial \dot{w}$	0.017
M_q	$\partial M/\partial q$	-93.391
M_{δ_e}	$\partial M/\partial \delta_e$	2.657
Z_{δ_e}	$\partial Z/\partial \delta_e$	-12.24

6 Stick fixed longitudinal motion

To examine the longitudinal motion of our vessel without any control input (controls fixed) when disturbed by a perturbation.

6.1 State variable representation

The linearized small-disturbance equations of motion are ordinary linear differential equations with constant coefficients. These equations can be written as a set of first-order differential equations, the state-space equations, and mathematically represented as: $\dot{x} = Ax + B\mu$ where x is the state vector and μ is the control vector. The matrices A e B contain the plane's dimensional stability derivatives, which have been evaluated through the help of the Xfoil software. Rewriting these equations of motion in the state space form yields:

$$\begin{bmatrix} \Delta\dot{u} \\ \Delta\dot{w} \\ \Delta\dot{q} \\ \Delta\dot{\theta} \end{bmatrix} = \begin{bmatrix} X_u & X_w & 0 & -g \\ Z_u & Z_w & u_0 & 0 \\ M_u + M_{\dot{w}}Z_w & M_w + M_{\dot{w}}Z_w & M_q + M_{\dot{w}}u_0 & 0 \\ 0 & 0 & 1 & 0 \end{bmatrix} \begin{bmatrix} \Delta u \\ \Delta w \\ \Delta q \\ \Delta\theta \end{bmatrix} + \begin{bmatrix} X_\delta \\ Z_\delta \\ M_\delta + M_{\dot{w}}Z_\delta \\ 0 \end{bmatrix} \begin{bmatrix} \Delta\delta \end{bmatrix}$$

The forces and moment derivatives in the matrices have been divided by the mass of the airplane or the moment of inertia, respectively, in the following manner:
$X_u = \partial X/\partial u/m$
$M_u = \partial X/\partial u/I_y$ and so forth.
The longitudinal stability derivatives in the stability matrix A have been summarized in the following table.

A_{ij}	j=1	j=2	j=3	j=4
i=1	-0.06924	1.293	0	-9.81
i=2	-2.886	-27.17	-5.111	0
i=3	0.001467	-0.001467	-203.9	0
i=4	0	0	1	0

(54)

The derivatives belonging to the control matrix B have been evaluated to be the following:

B_{ij}	j=1
i=1	-0.06924
i=2	-2.886
i=3	0.001467
i=4	0

(55)

6.2 Eigenvalues and Eigenvectors of the stability matrix

The homogeneous solution to equation can be obtained assuming a solution of the form $x = x_r e^{\lambda_r t}$ which substituted in $\dot{x} = Ax + B\mu$ leaves

$$[\lambda_r \mathbf{I} - \mathbf{A}]\mathbf{x}_r = 0$$

where $\mathbf{I}$ is the identity matrix.

$$\text{I}= \begin{bmatrix} 1 & 0 & 0 & 0 \\ 0 & 1 & 0 & 0 \\ 0 & 0 & 1 & 0 \\ 0 & 0 & 0 & 1 \end{bmatrix}$$

In order to have nontrivial solutions the determinant $|\lambda_r I - A|$ must be 0. The roots are the eigenvalues or characteristic roots. For this purpose the software MATLAB has been used to determine the eigenvalues. The eigenvectors themselves can be determined once the eigenvalues are known, using the following relation. $[\lambda_r \mathbf{I} - \mathbf{A}]\mathbf{P}_{ij} = 0$ where $\mathbf{P}_{ij}$ is the eigenvector corresponding to the ijth eigenvalue.

6.2.1 Eigenvalues

The eigenvalues for the stability matrix developed for this vessel are found to be

$$\lambda_1 = -0.0186 \tag{56}$$

$$\lambda_2 = -15.2460 \tag{57}$$

$$\lambda_{3/4} = -99.3572 \pm 10.1002i \tag{58}$$

Namely,two negative real values and two complex values which indicate respectively two exponentially decaying modes of motion and two damped oscillatory modes. These results are obtained with the help of the MATLAB software.

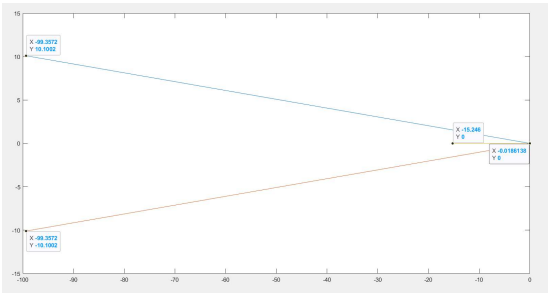

Figure 11: Complex eigenvalues of the stability matrix A

6.3 Short period approximation

An approximation to the short-period mode of motion can be obtained by assuming $\Delta u = 0$ and dropping the X-force equation from the set developed earlier. The longitudinal state-space equations, with the addition of the control input, reduce to:

$$\begin{bmatrix} \Delta\dot{w} \\ \Delta\dot{q} \end{bmatrix} = \begin{bmatrix} Z_w & u_0 \\ M_w + M_{\dot{w}} Z_w & M_q + M_{\dot{w}} u_0 \end{bmatrix} \begin{bmatrix} \Delta w \\ \Delta q \end{bmatrix} + \begin{bmatrix} Z_{\delta e} \\ M_\delta + M_{\dot{w}} Z_{\delta e} \end{bmatrix} \begin{bmatrix} \Delta\delta_e \end{bmatrix}$$

Nelson [1] suggests this equation to be written in terms of angle of attack by using the relationship: $\Delta\alpha = \frac{\Delta w}{u_0}$.

Furthermore, from the definition of $M_{\dot{\alpha}}$ is

$$M_\alpha = \frac{1}{Iy}\frac{\partial M}{\partial \alpha} = \frac{1}{I_y}\frac{\partial M}{\partial(\Delta w/u_0)} = \frac{u_0}{Iy}\frac{\partial M}{\partial w} = u_0 M_w \tag{59}$$

Similarly, it can be showed that:

$$Z_\alpha = u_0 Z_w \tag{60}$$

and

$$M_{\dot{\alpha}} = u_0 M_{\dot{w}} \tag{61}$$

$$\begin{bmatrix} \Delta\dot{\alpha} \\ \Delta\dot{q} \end{bmatrix} = \begin{bmatrix} \frac{Z_\alpha}{u_0} & 1 \\ M_\alpha + M_{\dot{\alpha}} \frac{Z_\alpha}{u_0} & M_q + M_{\dot{\alpha}} \end{bmatrix} \begin{bmatrix} \Delta\alpha \\ \Delta q \end{bmatrix} + \begin{bmatrix} \frac{Z_\delta}{u_0} \\ M_{\delta e} + M_{\dot{\alpha}} \frac{Z_{\delta e}}{u_0} \end{bmatrix} \begin{bmatrix} \Delta\delta_e \end{bmatrix}$$

The eigenvalues of the state equation can be determined by solving the equation $|\lambda I - A| = 0$

The characteristic equation for the determinant is

$$\lambda^2 - (M_q + M_{\dot{\alpha}} + \frac{Z_\alpha}{u_0})\lambda + M_q \frac{Z_\alpha}{u_0} - M_\alpha = 0 \tag{62}$$

The following approximated short period roots can be obtained by means of

$$\lambda_{sp} = (M_q + M_{\dot{\alpha}} + \frac{Z_\alpha}{u_0})/2 \pm [(M_q + M_{\dot{\alpha}} + \frac{Z_\alpha}{u_0})^2 - 4(M_q \frac{Z_\alpha}{u_0} - M_\alpha)]^{\frac{1}{2}}/2 \tag{63}$$

or, in terms of the damping and natural frequency

$$\xi_{sp} = -[M_q + M_{\dot{\alpha}} + \frac{Z_\alpha}{u_0}]/(2\omega_{sp}) \tag{64}$$

$$\omega_{sp} = [(M_q \frac{Z_\alpha}{u_0} - M_\alpha)]^{\frac{1}{2}} \tag{65}$$

This can be written in the form:

$$\lambda_{sp}^2 + \zeta\omega_n\lambda_{sp} + \omega_n^2 = 0 \tag{66}$$

Computing for the stability derivatives' value showed earlier, the two eigenvalues yielded by this short period approximation are:

$$\lambda_{1,2,sp} = -\zeta sp\omega sp \pm i\omega_{sp}\sqrt{1-\zeta sp^2} = \eta \pm i\omega = -99.87 \pm 9.072i \tag{67}$$

Follows a plot of the complex roots associated with the short period approximation

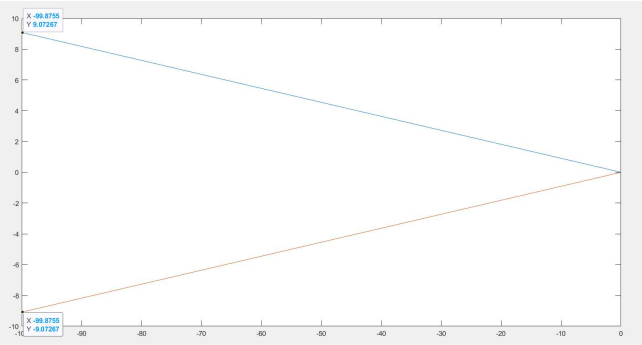

Figure 12: Complex short period roots of the short period approximation

Once the eigenvalues are known, we can derive period, time and number of cycles to half-amplitude, which are of great interest when evaluating the plant's free response.

$$Period = \frac{2\pi}{\omega} = 0.6925s \tag{68}$$

$$t_{1/2} = \frac{0.69}{|\eta|} = 0.0069s \tag{69}$$

$$N_{1/2} = \frac{t_{1/2}}{P} = 9.963e^{-}3 \tag{70}$$

6.4 Influence of stability derivatives on short period motion

Some interesting observations can be made at this point of the analysis. Graphically we can see the effect of stability derivatives on the complex eigenvalues of the short period roots. Increasing the static stability, represented by the negative value M_α (described earlier in the chapter about static stability) will increase the frequency of the short period mode.

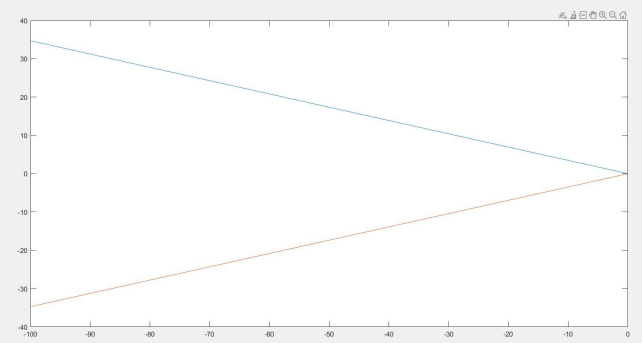

Figure 13: Roots of the short period approximation when M_α is increased tenfold

On the other hand, increasing $M_q + M_{\dot{\alpha}}$ affects the damping of the system enhancing it.

6.5 Short Period Dynamics

$$\begin{bmatrix}\Delta\dot{\alpha}\\ \Delta\dot{q}\end{bmatrix} = \begin{bmatrix}\frac{Z_\alpha}{u_0} & 1\\ M_\alpha + M_{\dot{\alpha}}\frac{Z_\alpha}{u_0} & M_q + M_{\dot{\alpha}}\end{bmatrix}\begin{bmatrix}\Delta\alpha\\ \Delta q\end{bmatrix} + \begin{bmatrix}\frac{Z_\delta}{u_0}\\ M_\delta + M_{\dot{\alpha}}\frac{Z_\delta}{u_0}\end{bmatrix}\begin{bmatrix}\Delta\delta\end{bmatrix} \tag{71}$$

Taking the Laplace transform of the state-space equations we have

$$(s - Z_\alpha/u_0)\Delta\alpha(s) - \Delta q(s) = Z_\delta/u_0\Delta\delta_e(s) \tag{72}$$

$$-(M_\alpha + M_{\dot{\alpha}}Z_\alpha/u_0)\Delta\alpha(s) + [s - (M_q + M_{\dot{\alpha}})]\Delta q(s) = (M_\delta + M_{\dot{\alpha}}Z_\delta/u_0)\Delta\delta_e \tag{73}$$

Dividing by $\Delta\delta_e$ we obtain two algebraic equations in terms of the transfer functions $\frac{\Delta\alpha(s)}{\Delta\delta_e(s)}$ and $\frac{\Delta q(s)}{\Delta\delta_e(s)}$:

$$(s - Z_\alpha/u_0)\frac{\Delta\alpha(s)}{\Delta\delta_e(s)} - \frac{\Delta q(s)}{\Delta\delta_e(s)} = Z_\delta/u_0 \tag{74}$$

$$-(M_\alpha + M_{\dot{\alpha}}Z_\alpha/u_0)\frac{\Delta\alpha(s)}{\Delta\delta_e} + [s - (M_q + M_{\dot{\alpha}})]\frac{\Delta q(s)}{\Delta\delta_e} = (M_\delta + M_{\dot{\alpha}}Z_\delta/u_0) \tag{75}$$

Dividing the equations by $\delta_e(s)$ we obtain a set of 2 equations in terms of the transfer functions $\frac{\Delta\alpha(s)}{\Delta\delta_e(s)}$ and $\frac{\Delta q(s)}{\Delta\delta_e(s)}$:

$$\begin{aligned}(s - \frac{Z_\alpha}{u_0})\frac{\Delta\alpha(s)}{\Delta\delta_e(s)} - \frac{\Delta q(s)}{\Delta\delta_e(s)} = \frac{Z_{\delta_e}}{u_0} - (M_\alpha + M_{\dot{\alpha}}Z_\alpha/u_0)\frac{\Delta\alpha(s)}{\Delta\delta_e(s)} + \\ + [s - (M_q + M_{\dot{\alpha}})]\frac{\Delta q(s)}{\Delta\delta_e(s)} = \\ = (M_\delta + M_{\dot{\alpha}}Z_\delta/u_0)\Delta\delta_e\end{aligned} \tag{76}$$

Solutions for $\frac{\Delta\alpha(s)}{\Delta\delta_e(s)}$ and $\frac{\Delta q(s)}{\Delta\delta_e(s)}$ can be achieved using Cramer's rule for systems of linear equations that have the same number of equations as variables. In this manner we are able to derive a relationship between the motion variables (pitch displacement θ and pitch rate q) and the control input. The transfer function for the change in pitch rate to the change in elevator angle is

$$\frac{\Delta\alpha(s)}{\Delta\delta_e(s)} = \frac{\begin{vmatrix} s - \frac{Z_\alpha}{u_0} & \frac{Z_{\delta_e}}{u_0} \\ -(M_\alpha + M_{\dot{\alpha}}\frac{Z_\alpha}{u_0}) & M_q + M_{\dot{\alpha}}\end{vmatrix}}{\begin{vmatrix} s - \frac{Z_\alpha}{u_0} & -1 \\ -(M_\alpha + M_{\dot{\alpha}}\frac{Z_\alpha}{u_0}) & s - (M_q + M_{\dot{\alpha}})\end{vmatrix}} = \frac{A_\alpha s + B_\alpha}{As^2 + Bs + C} \tag{77}$$

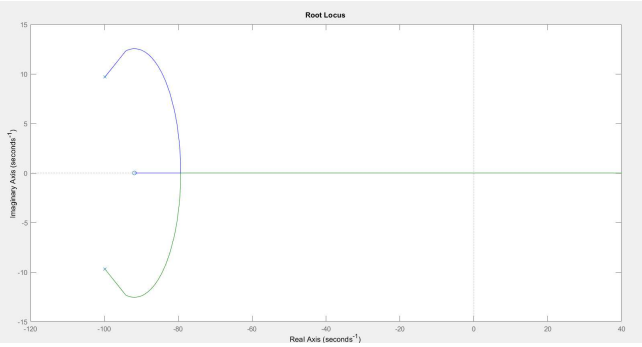

Figure 14: Root locus of the elevator angle to angle of attack transfer function

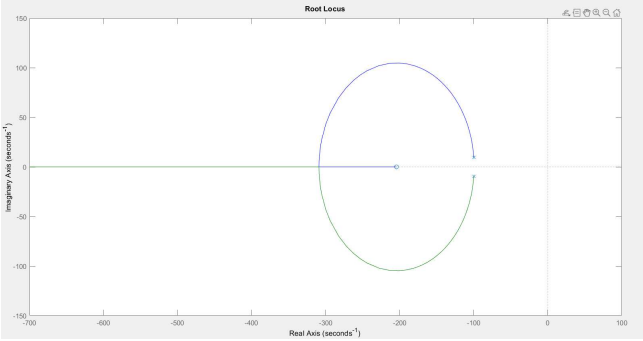

Figure 15: Root locus of the elevator angle to pitch rate transfer function

The transfer function for the change in angle of attack to the change in elevator angle is

$$\frac{\Delta q(s)}{\Delta \delta_e(s)} = \frac{\begin{vmatrix} \frac{Z_{\delta_e}}{u_0} & -1 \\ M_\alpha + M_{\dot{\alpha}} \frac{Z_\alpha}{u_0} & s - (M_q + M_{\dot{\alpha}}) \end{vmatrix}}{\begin{vmatrix} s - \frac{Z_\alpha}{u_0} & -1 - (M_\alpha + M_{\dot{\alpha}} \frac{Z_\alpha}{u_0}) & s - (M_q + M_{\dot{\alpha}}) \end{vmatrix}} = \frac{2.657s + 500.1}{s^2 + 199.8s + 10001} \tag{78}$$

The root locus of the $\frac{\Delta q}{\Delta \delta_e}$ transfer function was plotted with the help of the MATLAB software and are presented in the next images.

7 Pitch displacement autopilot

The transfer functions modeled previously for short period dynamics can be used to develop an autopilot for pitch displacement. In particular, bearing in mind the following relation $\Delta q = \Delta\dot{\theta}$, therefore $\Delta q(s) = s\Delta\theta(s)$. The following relation stands :

$$\frac{\Delta\theta}{\Delta\delta_e} = \frac{1}{s}\frac{\Delta q}{\Delta\delta_e} = \frac{A_q s + B_q}{s[As^2 + Bs + C]} = \frac{2.449s + 500.1}{s^3 + 199.6s^2 + 1.006e04s} \tag{79}$$

The plot of the root locus of this transfer function is the following:

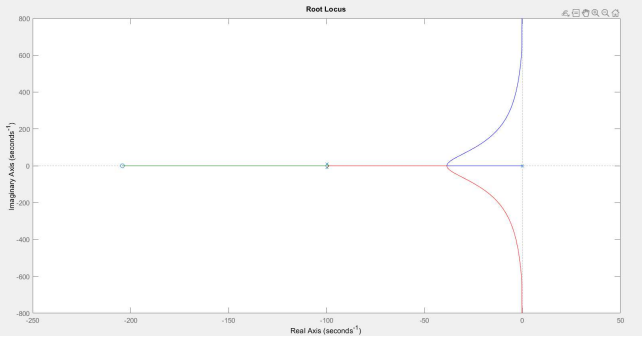

Figure 16: Root locus of the transfer function $\Delta\theta/\Delta\delta_e$

The system's pitch angle feedback loop can be represented in the following block diagram:

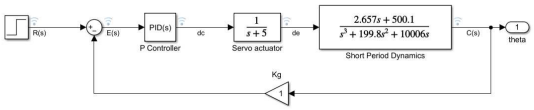

Figure 17: Block diagram representing the system with a PID controller

Were:

$R(s)$ is the reference input
$C(s) = E(s)G(s)$ is the output signal, in our case $\Delta\theta$
$E(s) = R(s) - C(s)$ is the error signal
$G(s) = C(s)/E(s)$ is the forward path transfer function

$G_s(s) = \frac{\Delta\delta_e}{E(s)}$ is the servo flap actuator transfer function
$H(s)$ is the feedback transfer function

For simplicity purposes the feedback gain k_g is set to 1, implying the use of an ideal gyroscope for the pitch angle measurement making the feedback transfer function $H(s) = 1$.

The servo motor modeled with a first order system, whose open loop transfer function is $G_s(s) = \frac{1}{sT}$ where T is the time constant and has been estimated to be $T = 0.2s$. When a unitary feedback loop is implemented in the servo architecture, the closed loop transfer function becomes:

$$G(s) = \frac{\Delta e(s)}{\Delta c(s)} = \frac{G_s(s)}{1 + G_s(s)} \tag{80}$$

or, as equivalently noted in the Simulink model:

$$G_s(s) = \frac{1}{s + 5} \tag{81}$$

The open-loop transfer function for the pitch dynamics will be the Laplace domain product of the servo transfer function and the short period dynamics previously presented.

$$G(s) = G_s(s)\frac{\Delta\theta}{\Delta\delta_e} = \frac{\Delta\delta_e}{E(s)}\frac{\Delta\theta}{\Delta\delta_e} \tag{82}$$

The closed loop transfer function for the system with a unitary feedback transfer function is:

$$\frac{C(s)}{R(s)} = \frac{G(s)H(s)}{1 + G(s)H(s)} \tag{83}$$

where the loop transfer function is identified by:

$$G(s)H(s) = \frac{\Delta\delta_e}{E(s)}\frac{\Delta\theta}{\Delta\delta_e} = \frac{2.449s + 500.1}{s^4 + 200.6s^3 + 1.026e04s^2 + 1.006e04s} \tag{84}$$

and the root locus is presented following.

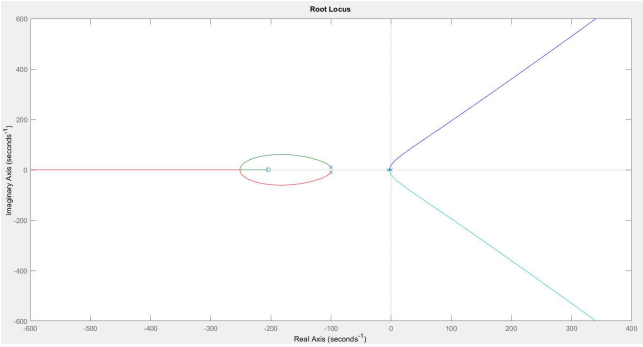

Figure 18: Loop transfer function locus

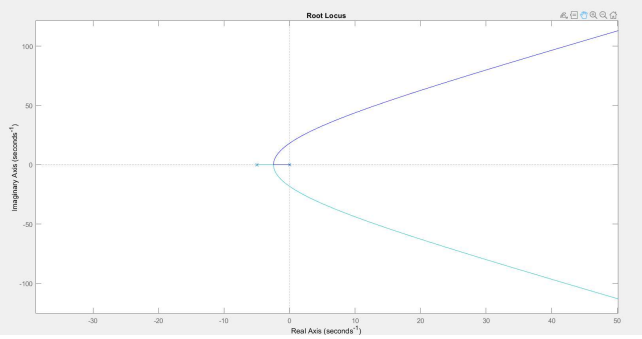

Figure 19: Zoom-in of the loop transfer function root locus

7.1 Control specifications/requirements

The control requirements for the system in study are:

overshoot $\leq 10\%$
$risetime \leq 1sec$

steady state error $\leq 2\%$
$settlingtime \leq 2sec$

7.2 PID Controller Proposal for a Pitch Displacement Autopilot

This design would benefit from the introduction of a controller to improve its natural performance, and a proposal for a PID type of controller was made using the Ziegler-Nichols method [7]. The general form of the PID transfer function

is $\frac{\Delta c}{\Delta e} = k_p + k_d s + \frac{k_i}{s}$;
k_p, k_i and k_d are the gains of the controller.

Adding a proportional gain k_p to the transfer function $G(s)H(s)$ allows us to determine the value of k_{p_u}, called ultimate gain, for witch the system becomes marginally stable. The gain at the crossover point can be estimated using the magnitude criteria:

$$\frac{|s + 204,2|k_p}{|s||s + 5||s^2 + 199.6s + 1.006e04|} = 1 \tag{85}$$

The root locus intersects the imaginary axis at $s = 8.17i$, which substituted in the previous equation yields :

$$k_{p_u} = 3852.6 \tag{86}$$

The period of the undamped oscillation period T_u can be found in the following manner:

$$T_u = \frac{2\pi}{\omega} = 0.77s \tag{87}$$

Once these parameters are known it is possible to evaluate the proportional, integral and derivative gains of the controller with the help of the relationships developed by Nelson[1].

$k_p = 2311$
$k_i = 6004$
$k_d = 222.48$
An alternative tuning proposal was carried out with the help of the Simulink software and has yielded the values:

$k_p = 623.78$
$k_i = 385.43$
$k_d = 102.06$

7.2.1 Steady State Error Evaluation

The error signal $E(s)$ can be expressed as $E(s) = \frac{R(s)}{1+G(s)H(s)}$ where $R(s)$ is the reference signal.

By evaluating the steady state error of the system with a given input we are able to assess its accuracy. Our system has a pole in the origin of magnitude, this making it a type 1 system. Practically, the type of the system affects its capability of reaching a desired reference value accurately unless properly controlled. In the case of study, the type of the system will guarantee null error for step unitary reference inputs even while only proportional and derivative (PD) control is applied, but will show a steady state error for ramp inputs unless integral control is applied. [img proportional contol error]The value of the steady state error can be evaluated by means of the final value theorem, which states:

$$e_{ss} = \lim_{t\to\infty} e(t) = \lim_{s\to 0} sE(s) \tag{88}$$

If we take a step input $r(t) = Au(t)$, whose Laplace transform is $R(s) = A/s$, the previous limit becomes

$$\begin{aligned} e_{ss} = \lim_{s\to 0} sE(s) = \lim_{s\to 0} \frac{s(A/s)}{1 + G(s)H(s)} = \\ = \lim_{s\to 0} \frac{A}{1 + G(s)H(s)} = \frac{A}{1 + \lim_{s\to 0} G(s)H(s)} \end{aligned} \tag{89}$$

where $K_p = \lim_{s\to 0} G(s)H(s)$ takes the name of positional error constant. In our case $K_p = \infty$ thanks to the transfer function pole in zero.

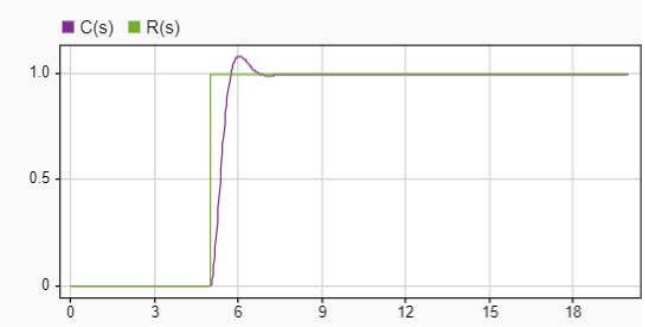

Figure 20: Response to ramp input with PD controller

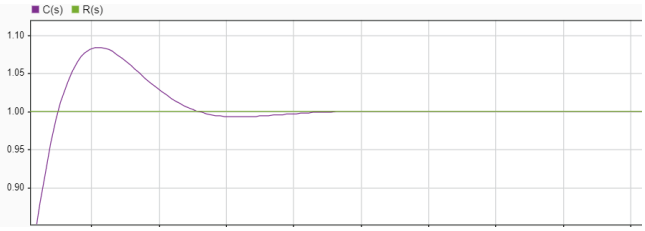

Figure 21: Zoom-in of the response to ramp input, showing constant steady state error

If we take a step input $r(t) = At$, whose Laplace transform is $R(s) = A/s^2$, the limit becomes

In our case, we can appreciate an elimination of the transfer function pole in zero, and hence $K_v = 0.049$ yields a steady state error $E(s) = \frac{A}{0.049}$ which is proportional to the magnitude of the ramp input, or in other words the steepness of the ramp.

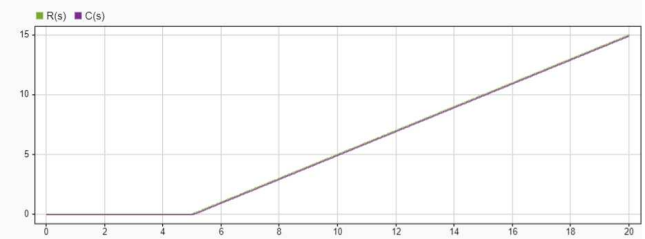

Figure 22: Response to ramp input with PD controller

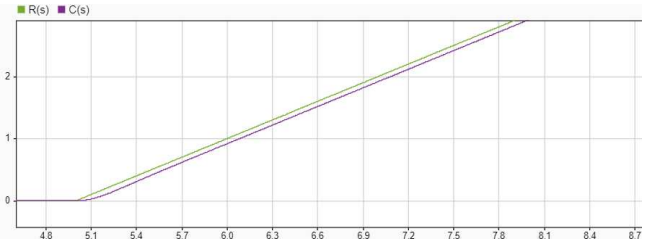

Figure 23: Zoom-in of the response to ramp input, showing constant steady state error

8 Conclusions

The representation of the model as carried out in this work is satisfactory for the purpose of longitudinal stability assessment, and the underlying theory presented was kept to as straightforward as possible. From the previous evaluation we can see that the proposed feedback control architecture meets the requirements in terms of overshoot, rise time and steady state error. Different proposals for control architectures, can also prove effective. We have seen that a proportional-derivative controller would also meet control requirements while tracing a step reference, while PID guarantees better results for more complex reference signals. An alternate proposal could be made for this project's pitch control architecture, namely by implementing a pitch rate controller in an cascaded inner loop for the purpose of controlling more efficiently the pitch attitude, and this will be kept in consideration for a further development of this work. The position of the mass of the only crew is an aspect which has been overlooked in this work, and has been simply modeled as a fixed point mass. The crew has a crucial role on this type of vessel, providing restoring moment both in the pitch and in the roll direction, that is around the Y and X body axis. This behaviour is used do interact with the center of gravity and compensate in an intuitive way to dynamical behaviour of the vessel. This intuitive corrections are of the uttermost importance during the transition phase, between the buoyant and flying configuration, and whenever there is a variation in the windspeed, thus generating a variation in both propulsive forces and heeling momentum. The compensation is left solely at the sailor which is in charge of balancing the wind induced moments, and hence they would greatly benefit from having some insight on the way their positioning affects the flying behaviour of the vessel. In the work of Eggert [2]a PID controller is also used to implement the position of the crew variable: this controller has the aim of mimicking the sailor's intuitive corrections within the viable envelope for crew mobility. Investigating this matter more in depth would yield some valuable practical results regarding crew positioning at different speeds and gaits.

References

[1] Robert C. Nelson (1989) *Flight Stability and Automatic Control*, McGraw-Hill, 2nd ed.

[2] Fabio Eggert (2008) *Dynamics and Stability of a Hydrofoiling International Moth with a Dynamic Velocity Prediction Program*, Dynamics of Maritime Systems Technische Universität Berlin.

[3] Michael V. Cook (2007)*Flight Dynamics Principles, Second Edition A Linear Systems Approach to Aircraft Stability and Control*, Elsevier Aerospace Engineering, 2nd ed.

[4] Sighard F. Hoerner (2006)*Fluid-Dynamic Lift Practical Information on Aerodynamic and Hydrodynamic Lift.*

[5] Chris Miller, *Control System for International Moth on Hydrofoils* Glasgow University

[6] Christian Bögle (2010),*Evaluation of the Performance of a Hydro-Foiled Moth by Stability and Force Balance Criteria*, Department of Ocean Engineering and Naval Architecture TU-Berlin, Berlin, Germany

[7] Astrom-Hagglund(1988), *Automatic Tuning of PID Controllers*, Instrument Society of America

[8] Rob Greenhalgh (2019), *International Moth Speed Guide*, North Sails, `https://www.northsails.com/sailing/it/resources/north-sails-international-moth-speed-guide-2`

[9] International Moth Class Association (2017), *International Moth Class Rules*,`https://www.sailing.org`

[10] MetisVela UniPD student project, `http://metisvela.dii.unipd.it`

[11] SuMoth Foiling Challenge, http://sumoth.org

[12] XFLR5 analysis tool for airfoils, wings and planes at low Reynolds Numbers, `http://www.xflr5.tech/xflr5.htm`

[13] MATLAB®, `https://it.mathworks.com/products/matlab.html`

[14] Simulink environment,`https://it.mathworks.com/products/simulink.html`